Cretaceous accretionary complex related to Okhotsk-Chukotka Subduction, Omgon Range, Western Kamchatka, Russian Far East

Alexey Soloviev[a,*], John I. Garver[b], Galina Ledneva[a]

[a]Geological Institute, Russian Academy of Sciences, Moscow, Russia
[b]Union College, Geology Department, Schenectady, NY 12308, USA

Abstract

The Omgon Range of Western Kamchatka contains a mid to Upper Cretaceous sequence of flysch with tectonic inclusions of Jurassic–Cretaceous oceanic rocks inferred to have been imbricated together in an accretionary prism. These rocks were tectonically juxtaposed during the Cretaceous in a mélange that contains a number of elements but mainly includes: (1) Middle Jurassic–Lower Cretaceous volcanic rocks formed in an oceanic and/or marginal sea environment; and (2) Albian–Campanian terrigenous turbidites made of quartz-rich clastic sediments that accumulated near a continental-margin. The oceanic rocks are inferred to have been tectonically incorporated into the continental terrigenous unit by offscraping during subduction. The accretionary prism resulted from subduction of the Pacific paleo-oceanic plate (Izanagi) under the Eurasian continental margin, which ultimately caused volcanism in the inboard Okhotsk-Chukotka volcanic belt. Internal imbrication was completed by the Maastrichtian ($\sim$70 Ma) as indicated by apatite fission-track ages that record cooling and exhumation of this crustal block. The Omgon accretionary wedge originated in a similar geodynamic setting and same time as the Yanranai (northern Korayk), Tonino–Aniva (southeastern Sakhalin), Hidaka (northeastern Japan) and Cretaceous part of the Shimanto belt (southwestern Japan). The similarities of ages, lithology, and tectonic setting suggest that the Omgon accretionary wedge was part of a paleo-subduction zone along the Eurasian margin during the mid to Late Cretaceous.
© 2005 Elsevier Ltd. All rights reserved.

Keywords: Fission-track; Accretionary wedge; Mélange, Cretaceous; Kamchatka

1. Introduction

Northeast Asia includes oceanic and arc terranes of Paleozoic to Cenozoic age that have been swept into the margin from the Late Jurassic to Tertiary (Stavsky et al., 1990; Nokleberg et al., 1998). A dominant feature of the geology along this margin is the Cretaceous Okhotsk-Chukotka volcanic belt (OCVB), which is a continental arc built on part of this collage of terranes. The OCVB represents a laterally extensive Andean-style arc that persisted along the southern margin of the western and northern edge of what is now the modern limit of the Sea of Okhotsk and Bering shelf (Filatova, 1988; Nokleberg et al., 1998). The duration of magmatic activity in OCVB is

debated but generally thought to include the Middle Albian to Campanian time (Belyy, 1977, 1994; Filatova, 1988; Zonenshain et al., 1990; Kotlyar et al., 2001). It sits on a collage of terranes that were assembled prior to the Albian. Calc-alkaline volcanic rocks from the exterior zone show that magmatism occurred locally between 86 and 81 Ma, and basaltic rocks with within-plate geochemical affinities yielded ages ranging from 78 to 74 Ma (Hourigan, 2003). The outboard forearc to this continental arc is less well defined and only partly exposed due to cover by adjacent offshore marine basins and younger strata.

One important question for regional tectonic reconstructions is the continuity and lateral extent of subduction accretion associated with this important continental arc, and this question highlights two primary motivations for our focus on these units. First, we are interested in understanding the history of long-term subduction accretion of oceanic material to the paleomargin. This material includes

---

* Corresponding author. Fax: +7 95 953 55 90.
E-mail address: solov@ilran.ru (A. Soloviev).

a number of oceanic complexes and turbiditic assemblages that record the dispersal of petrotectonic elements along the margin, mostly northward on Pacific plates. Second, we are interested in understanding the continuity of petrotectonic assemblages along the paleomargin, which has been disrupted and covered by younger elements. One of those elements is normal faulting in the Sea of Okhotsk, which has disrupted accreted assemblages through progressive north- to south-extension and wholesale crustal thinning. Another is the deposition of volcanic and sedimentary sequences related to subsequent arc-related volcanism, which is represented by the modern Kamchatka-Kurile arc. Together, the continuity of the Cretaceous paleomargin has been obscured and therefore correlation of disparate blocks has been challenging.

A detailed understanding of the lithology, structural history, age and origin of internal blocks, and thermal history of accretionary complexes can provide important insight into the their setting and mode of emplacement. One distinctive attribute of accretionary complexes is their thermal history. Fission-track studies of exposed accretionary wedges have been carried out in a number of places in the Pacific Rim including southwest Japan (Shimanto belt; see Hasebe et al., 1993; Hasebe and Tagami, 2001), and the west coast of North America (Franciscan Complex; Dumitru, 1989; and Olympic Subduction Complex; Brandon and Vance, 1992; Brandon et al., 1998; Stewart and Brandon, 2004). The accretionary wedge complexes related to the OCVB subduction are poorly known because much of the likely outcrop belt is offshore in the Bering Sea and Sea of Okhotsk, or in a remote and logistically complicated region on the northern Kamchatka Peninsula. Therefore, little is know of these units, which we believe are a crucial to paleotectonic reconstructions in this area.

Our research is focused on rocks of very limited geographic extent in the Omgon Range, which are some of the westernmost pre-Tertiary rocks on the Kamchatka Peninsula (Fig. 1). In fact there are no other rocks like this on the Kamchatka peninsula, so they provide a glimpse of what is largely buried geology in this area. Our study is based on mapping, structural analysis, geochemistry of included blocks, and fission-track dating of detrital zircon and apatite from sandstones of the flysch complex. These studies resulted in the conclusion that the rock complexes of the Omgon Range are fragments of a Cretaceous accretionary prism presumably related to OCVB subduction. As such, this small isolated exposure,
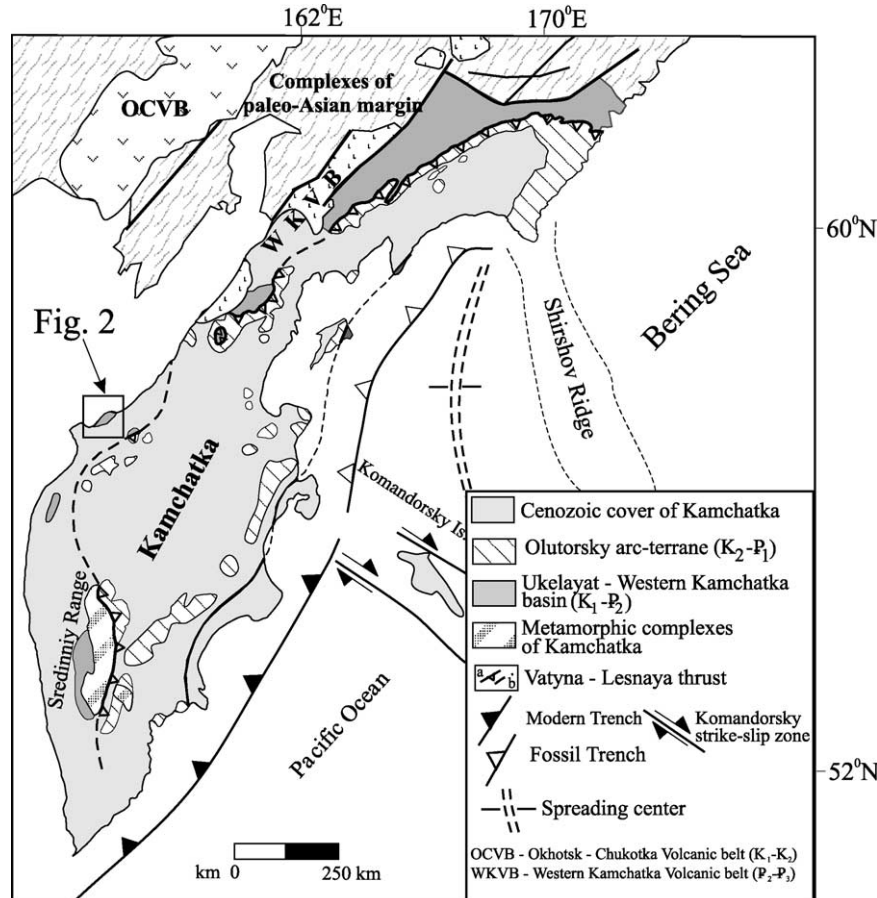

Fig. 1. General geological setting of Kamchatka in the Russian Far East.

largely surrounded by Tertiary sedimentary strata, is perhaps the single remaining onland exposure of this tectonostratigraphic unit.

2. Geological overview

The geology of the Kamchatka Peninsula is dominated by the Neogene arc and related cover rocks. Pre-Tertiary rocks in Kamchatka generally occur as isolated exposures, but are present throughout the Peninsula. Pre-Tertiary rocks in Western Kamchatka are uncommon and exposed as widely scattered, isolated remote exposures that are very difficult to access due to limited infrastructure. Although pre-Tertiary rocks are exposed along the western coast of Kamchatka, rocks in the Omgon Range are quite distinct from others in age and structure (Fig. 1), and have long been regarded as unique.

The Omgon Peninsula juts out into the poorly understood Sea of Okhotsk, and therefore the rocks likely provide insight into the evolution of this basin. The Sea of Okhotsk is floored almost exclusively by thinned continental crust. Relatively little is known of the age and mechanism of formation of the Sea of Okhotsk because the nature of basement lithologies is almost completely unknown (Hourigan, 2003). Crustal rocks that floor the Sea of Okhotsk have been considered an example of a: (1) captured oceanic plateau (Watson and Fujita, 1985; Bogdanov and Dobretsov, 2002); (2) accreted microcontinent block (Parfenov and Natal'in, 1977; Zonenshain et al., 1990; Konstantinovskaia, 2001), or (3) extended continental framework of accreted terranes (Hourigan, 2003). Either way, the lack of real data has allowed flexibility of geological models. One of the biggest problems is that basement rock has never been drilled, so most of what is known is inferred from seismic data or dredging, but dredged material is regarded as suspect due to possible ice-rafting.

The collided-block model holds that an allochthonous sialic or oceanic plateau collided with the margin of northeastern Asia in the Late Cretaceous, resulting in the cessation of magmatism in the Andean-style Okhotsk-Chukotka belt (Parfenov and Natal'in, 1977; Zonenshain et al., 1990; Konstantinovskaia, 2001; Bogdanov and Dobretsov, 2002). In some models, the microcontinental block forms the basement of the Sea of Okhotsk and extends on land on the Kamchatka Peninsula. One such place where this rock is exposed onshore may be in the metamorphic rocks in the Sredinniy Range (Khanchuk, 1985). One new hypothesis is that the Omgon-Palana belt (north and west of Sredinniy) is a collision zone separating the Sea of Okhotsk plate from the West Kamchatka microplate (Bogdanov and Chekhovich, 2002). They surmise that a fragment of an ancient oceanic plateau makes up the Sea of Okhotsk microplate, while the West Kamchatka plate is quasi-continental crust (Bogdanov and Chekhovich, 2002). A

back-arc extensional model for the origin of the Sea of Okhotsk has recently been proposed, where basement rocks are inferred to be comprised of a variety of Mesozoic terranes in a south-propagating extensional zone that has progressively extended since the Eocene (Hourigan, 2003).

Previous work has revealed that rocks of the Omgon Range include an imbricated complex of volcanic, siliceous, and carbonate rocks (Lower Cretaceous Kingiveem Formation) and a terrigenous complex (Lower to Upper Cretaceous Omgon Series) (Markovsky, 1989). The volcanic–siliceous rock complex (Kingiveem Formation) has been dated as Middle Jurassic (Bajocian-Bathonian) to Lower Cretaceous (Lower Aptian) based on radiolarians (Bondarenko and Sokolkov, 1990; Bogdanov et al., 1991; Vishnevskaya et al., 1999). Flora and fauna from the Omgon Series indicate that accumulation of the terrigenous rocks occurred in the mid Cretaceous (in this case, Albian to Santonian) (Vlasov, 1964).

3. Geological structure of the Omgon Range

Following our mapping and field investigations, we subdivide Mesozoic rocks of the Omgon Range (Fig. 2) into a volcanic complex and a terrigenous complex, which are tectonically interleaved. The volcanic complex consists of pillow and massive aphyric, clinopyroxene–plagioclase and plagioclase–microphyric, commonly amygdaloidal, basalt, dolerite-basalt, and dolerite enclosing interlayers and lenses of chert, siliceous mudstone, and, rarely, pelagic limestone. All rocks of the volcanic complex make up fault-bounded blocks and sedimentary slide blocks in the rocks of the terrigenous complex. The terrigenous complex consists of sandstones, siltstones, and mudstones, commonly with a flysch-like alternation and interbedded thick conglomerate beds.

Several tectonic slices have been mapped in the southern segment of the Omgon Range. These slices consist of volcanic rocks in panels that dip almost exclusively to the northwest (Fig. 2). Structural observations at site 3 (Fig. 2) reveal that both the volcanic and the terrigenous rocks dip predominantly to the northwest (Fig. 3E) and faults that bound the slides and blocks dip to the west (Fig. 3F). An oblique relationship between the average fold axis (π-axis) and fault strike probably reflects a strike-slip component of displacement along a master fault.

While most folds in the Omgon rocks verge north and northwest, there is generally a chaotic distribution of fold axes (Figs. 2 and 3C,D). This observation may suggest that the southern part of site 2 experienced rotation because vergence differs dramatically from vergence of rocks at sites 3 and 1. Block rotation may be additional evidence for strike-slip displacement. Two kilometers south of Cape Promezhutochny, rocks of the terrigenous complex are truncated by a nearly vertical, northeast-trending fault with a strike-slip component (see Fig. 2), but the direction of
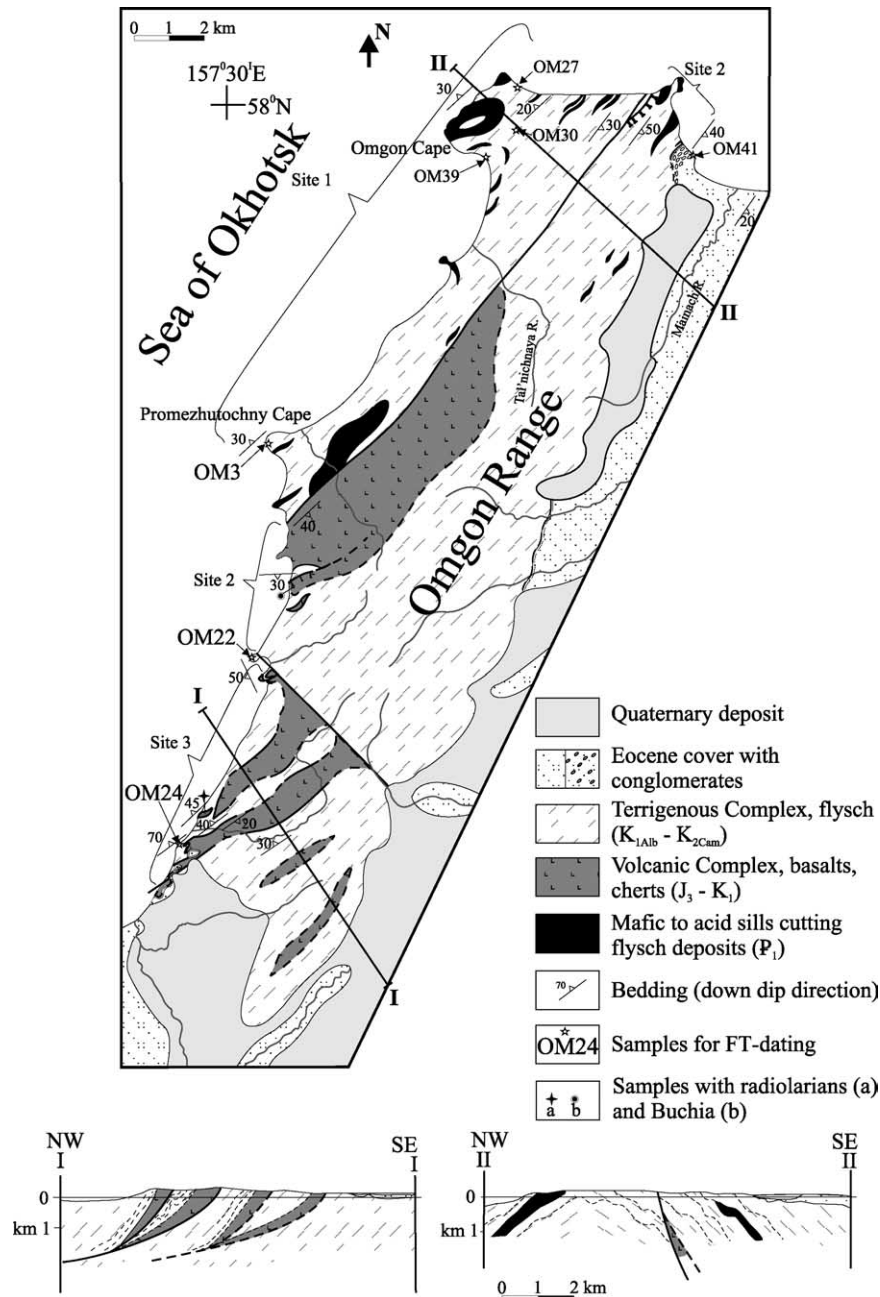
Fig. 2. Schematic geological map of the Omgon Range (Western Kamchatka) with simplified cross-sections.

strike-slip movement is not clear. Terrigenous rocks do not enclose any blocks of volcanic rocks north of this fault (site 1; see Fig. 2). Competent terrigenous rocks (sandstones and conglomerates) make up a large southeast–northwest-trending anticline (Fig. 3A) and more plastic thin-bedded shale in the core of the anticline are isoclinally folded with chaotically oriented fold axes (Fig. 3B). This pattern might have been produced by deformation of poorly lithified sediments or disharmonic folding. Numerous sills of gabbro, diorite, quartz diorite, granodiorite, and leucocratic granite, as well as quartz monzonite and granite–porphyry,

cut the rocks of the terrigenous complex at site 1 (Ledneva, 2001).

Non-marine, coal-bearing strata of the Middle Eocene Snatol Formation unconformably overlies the deformed and folded Mesozoic rocks (Gladenkov et al., 1991). This sharp angular unconformity between the terrigenous complex and the Eocene rocks has been described in the northern part of the Omgon Range (site 2, Fig. 2). Here, basal conglomerates consist of lithologies typical of the underlying pre-Tertiary rocks of the Omgon Range (volcanic and terrigenous rocks) and of the crosscutting sills. The Snatol Formation is folded
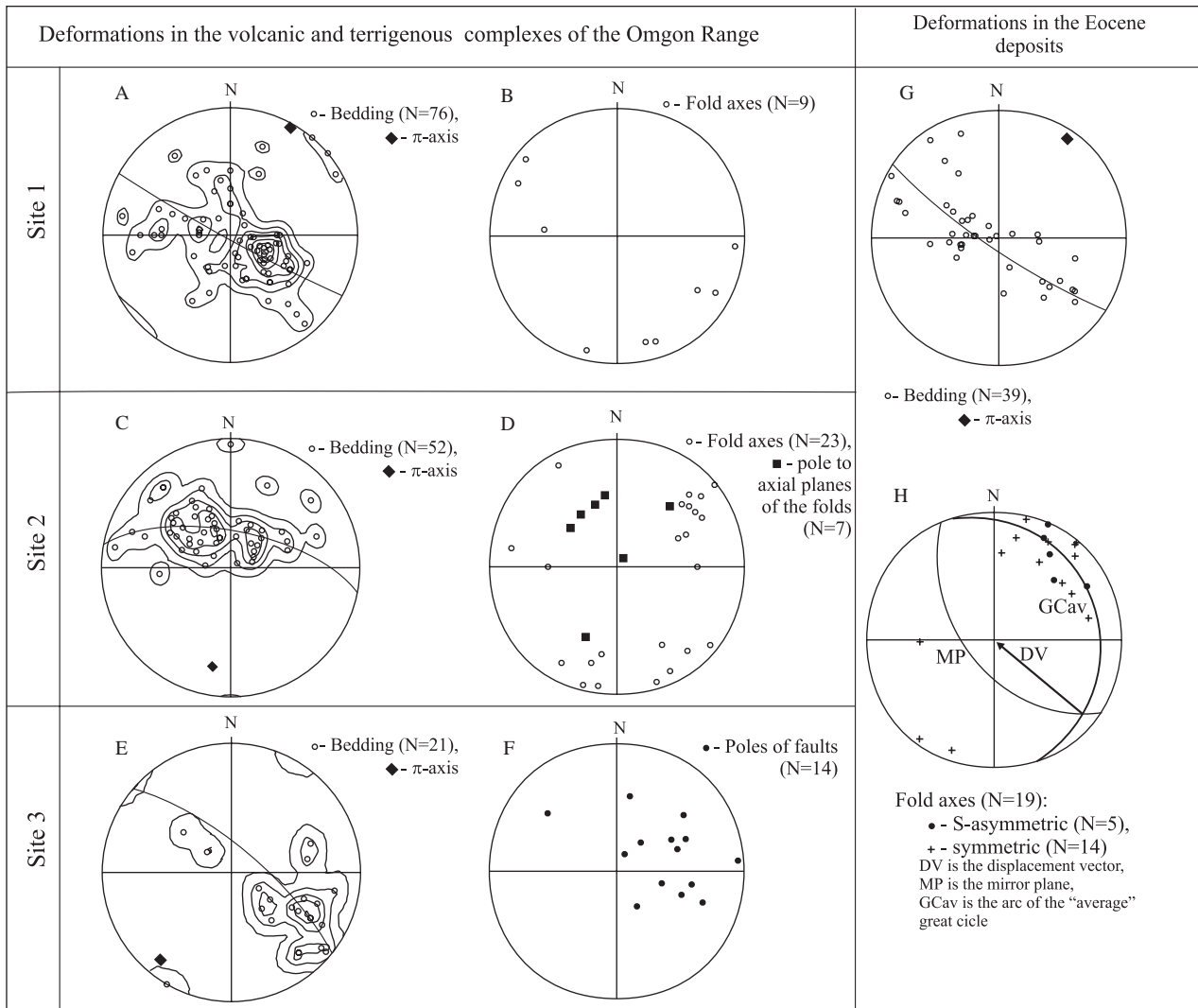
Fig. 3. Results of the structural–kinematic analysis of rock complexes in the Omgon Range (West Kamchatka). A–H are stereonets of various structural elements: A and B are for site 1 (Fig. 2): A, bedding planes; B, fold axes; C and D are for site 2 (Fig. 2): C, bedding planes; D, axial planes and axes of folds; E and F are for site 3 (Fig. 2): E, bedding planes; F, faults; G and H are for the Eocene deposits (Fig. 2): G, bedding planes; H, axes of asymmetric and symmetric folds. The linear and planar elements are shown with poles on a Schmidt net as projections on the lower hemisphere. N is the number of the structural elements of this type used for plotting the diagrams.

near the contact into tight to isoclinal folds with a northwest vergence (Fig. 3G). These asymmetric folds suggest a local displacement of the Eocene deposits northwestward (Fig. 3H). The folding of the Tertiary deposits becomes less intense with distance from the pre-Cenozoic rocks, and 1.5 km east of the mouth of the Mainach River, these deposits are folded in a gentle east-dipping monocline (Fig. 2).

These structural observations indicate that rocks in the Omgon Range experienced at least two deformations. The younger deformation must be post-Middle Eocene, and it resulted in the folding of the Middle Eocene rocks (and the underlying sequences), with the principal axis of contraction oriented southeast–northwest (Fig. 3G,H). The older deformation must be pre-Eocene, as this is the age of rocks that rest above the unconformity. The tectonic interleaving of the terrigenous and volcanic rocks likely

occurred during this first stage. The deformed rocks are Albian–Santonian, and because deformation may have been contemporaneous with deposition of the terrigenous rocks, we suspect that at least some of the earlier deformation occurred before Eocene deformation.

4. Composition and age of the rocks in the Omgon Range

4.1. Volcanic complex

The volcanic complex consists of sheets of pillow and massive, commonly amygdaloidal, basalt, ophitic dolerite, and dolerite enclosing interlayers and lenses of chert, siliceous mudstone, and minor limestone. Basalts at the top of sheets are represented by aphyric, clinopyroxene–

plagioclase–and plagioclase–microphyric varieties. They display sheaf-like and, more rarely, hyalopilitic and vitrophyric textures in the groundmass. Glass is completely replaced by an aggregate of light-green chlorite and finely disseminated magnetite; there are a few spilitized rocks. The central and basal parts of the sheets consist of well-crystallized, medium-grained doleritic basalts and dolerites composed of elongated and tabular plagioclase crystals and idiomorphic and subhedral crystals of clinopyroxene and magnetite, the magnetite locally forming accumulations. Small plagioclase laths are locally enclosed in larger clinopyroxene crystals. The interstices between these crystals are filled with an aggregate of radiated-axial chlorite and finely disseminated magnetite. The rocks have a doleritic texture. Clinopyroxene crystals are fresh, while plagioclase crystals are almost completely replaced with saussurite, and the magnetite locally shows evidence of oxidation. Amygdules in the basalts are filled with various minerals, carbonate and carbonate + magnetite being most common, and the association of carbonate + quartz or alkaline chlorite is less common. Veinlets in fractured rocks are filled with the same minerals and, more rarely, with tremolite, which indicates a supply of carbonate, silica, and alkalis. The discovery of exfoliation tuffs in the basalt sheets, as well as the presence of interlayers and lenses of chert, siliceous mudstone, and limestone, suggests that these basalts erupted in a subaqueous environment. The volcanic rocks have been weakly metamorphosed under low-temperature and low-pressure conditions.

The rocks examined showed high loss on ignition (LOI = 4.55–12.44%) (Table 1), as well as metamorphic alteration. Both observations preclude using most of the mobile elements for reconstructing the geodynamic conditions that existed during emplacement of the volcanic rocks. The concentrations of SiO_2, MgO, and Fe_2O_3 decline drastically with increasing LOI, which suggests that these components have been removed during alteration. However, the variations in the Fe_2O_3 and MgO abundances as a function of the LOI values are identical, implying that ratios between these components are essentially unmodified.

Variations in the contents of major- and trace-elements vary with the Mg# ($100 \times Mg/(Mg + Fe_{total})$) and allow us to distinguish two petrologic types of basalt: (a) poorly and moderately differentiated basalts (MgO = 9.12–7.29%) with normal iron content (Fe*/Mg = 1.17–1.69); and (b) highly differentiated basalts (MgO = 4.12–4.28%) with an elevated iron content (FeO*/MgO = 2.07–3.19). The behavior of major and trace elements in both of the recognized groups of rocks is compatible with crystallization from a melt with increasing differentiation of olivine + clinopyroxene + plagioclase and clinopyroxene + plagioclase + magnetite.

The Na_2O and K_2O contents and the high FeO*/MgO ratios suggest that the volcanic rocks of both types are close to the tholeiite series. Despite differences in some petrochemical-specific features, basalts with normal and elevated iron contents belong to the same geochemical type.

Basalts of both types are highly depleted in LREE relative to HREE ($(La/Yb)_N$ = 0.37–0.86 and 0.42–0.65, respectively) and have uniform Zr/Y (1.24–2.76 and 2.28–2.95) and Zr/Sm (23.5–27.7 and 25.5–30.2) ratios (Table 1). These parameters, together with discrimination diagrams (Fig. 4), place them close to N-MORB type basalts from oceanic spreading centers (and/or from those of marginal seas). Regionally these are similar to the Upper Jurassic–Lower Cretaceous N-MORB exposed at Cape Povorotny (Taigonos Peninsula) and in the Talovskie Mountains (northern Koryak) (Khanchuk et al., 1990; Grigor'ev et al., 1995; Sokolov et al., 2001; Silantyev et al., 2000).

4.2. Age of the volcanic complex

Previous work has confirmed the age of the volcanic rocks in the Omgon Range as Middle Jurassic–Early Cretaceous based on radiolarians from interbedded chert (Bondarenko and Sokolkov, 1990; Bogdanov et al., 1991; Vishnevskaya et al., 1999). We collected our own samples of siliceous rocks and undertook our own radiolarian analysis (Soloviev et al., 2001), and these indicate a Late Jurassic–Early Cretaceous age for the host rocks (determinations by T.N. Palechek). Buchia from this unit are Valanginian in age for siliceous rocks from the volcanic complex (Buchia inflata (Lahusen) and Buchia sublaevis (Keyserling) identified by V.A. Zakharov) (see Kirillova and Kiriyanova, 2003).

4.3. Terrigenous complex

Sandstones of the terrigenous complex are poorly sorted, angular graywackes. The sandstones are quartz–feldspar- and feldspar–quartz graywackes (Shutov et al., 1972). Various volcanic rock fragments and mudstone fragments are present among the rock fragments. Basalt, andesite, and rhyodacite fragments occur among the volcanic rock fragments, as well as fragments of devitrified glass. Mudstone fragments are especially common (up to 25%) among the sedimentary rock clasts. Second in abundance are sedimentary rock fragments consisting of a fine-grained, tuffaceous material. Siliceous sedimentary rock fragments (i.e. chert) are relatively rare (1–4%). The sediments also contain a minor, but common occurrence of dispersed coalified plant detritus. Fragments of metamorphic rock fragments (quartzite and mica schist) are rare (less than 3%), although they occur in all samples investigated. The overall composition suggests derivation from a dissected volcanic arc as discussed by Shapiro et al. (2001).

The specific chemical features of mudstones from the flysch succession support the conclusion that the clastic rocks were derived from a dissected continental volcanic arc (Table 2). The mudrocks are comparable, in terms of the abundance of HFS lithophile elements, as well as intermediate and heavy rare-earth elements (REE), with the average post-Archean shale (PAAS), whose

Table 1
Major and trace element contents in basalts from volcanic complex (the Omgon Range)

Sample	O-1/98	O-2/98	O-7/98	O-9/98	O-12/98	O-14/98	O-25/98
Major oxides (wt%)							
SiO_2	47.31	49.91	43.63	43.88	44.53	48.12	46.66
TiO_2	1.31	1.65	1.86	1.03	1.48	1.08	1.43
Al_2O_3	14.00	12.81	13.04	15.41	13.68	14.40	12.85
Fe_2O_3	13.87	9.07	10.22	10.81	12.23	12.26	13.49
MnO	0.16	0.16	0.23	0.22	0.19	0.18	0.17
MgO	7.40	3.94	3.67	8.31	6.82	8.08	3.81
CaO	7.91	10.73	12.25	7.94	12.04	8.50	9.62
Na_2O	2.08	3.56	3.46	3.00	2.20	2.30	3.40
K_2O	0.30	0.09	0.36	0.39	0.32	0.57	0.48
P_2O_5	0.17	0.17	0.21	0.14	0.16	0.15	0.14
LOI	5.81	8.58	12.44	9.73	6.78	4.55	8.63
Sum	100.32	100.68	101.38	100.86	100.43	100.20	100.69
#Mg	51.39	46.28	41.57	60.38	52.50	56.64	35.88
Trace and rare-earth elements (ppm)							
Sc	48	42	47	48	50	48	50
V	312	371	376	266	354	289	331
Cr	216	176	148	344	118	263	93
Co	49	55	39	65	50	46	34
Ni	97	129	67	171	101	117	76
Cu	148	138	70	125	167	135	72
Zn	75	92	116	74	86	72	81
Rb	3.6	0.7	5.1	10.1	6.6	9.5	12.5
Sr	136	116	138	215	171	497	116
Y	24	37	42	20	35	27	31
Zr	66	88	124	54	81	53	70
Nb	1.41	1.90		0.99	1.57	1.00	1.23
Ta	0.12	0.14		0.08	0.11	0.06	0.09
Ba	105	112	133	201	187	305	172
Hf	1.9	2.4	3.4	1.5	2.3	1.5	2.0
W	0.2	0.1	2.3	0.2	0.1	0.1	0.2
Pb	0.52	0.77	0.76	1.96	0.55	0.35	1.16
Th	0.09	0.18	0.20	0.09	0.11	0.06	0.12
U	0.03	0.12	0.59	0.06	0.18	0.03	0.60
La	1.86	2.41	3.72	2.48	2.14	1.34	2.07
Ce	6.30	8.09	11.45	7.01	7.36	4.72	6.88
Pr	1.11	1.43	1.98	1.11	1.36	0.88	1.26
Nd	6.32	8.43	11.17	5.92	8.37	5.46	7.13
Sm	2.39	3.20	4.11	2.18	3.20	2.25	2.76
Eu	0.89	1.11	1.32	0.86	1.17	0.88	1.02
Gd	3.29	4.50	5.57	2.89	4.57	3.36	3.96
Tb	0.59	0.85	0.98	0.53	0.85	0.61	0.75
Dy	4.07	5.81	6.65	3.48	5.76	4.18	5.17
Ho	0.94	1.36	1.55	0.78	1.35	1.00	1.18
Er	2.63	3.78	4.23	2.05	3.62	2.70	3.38
Tm	0.38	0.57	0.62	0.30	0.54	0.39	0.49
Yb	2.59	3.78	3.87	1.95	3.42	2.46	3.31
Lu	0.39	0.57	0.56	0.28	0.52	0.38	0.49

Notes. Mg#$=100 \times Mg^{2+}/(Mg^{2+} + Fe^{2+})$. The samples were crushed and powdered at the Laboratory of Miralogical and Fission-track analyses at the Geological Institute, RAS using the jaw crusher, vibrating cup mill and jasper mortar. The major- and trace-element contents were determined by X-ray fluorescence at the United Institute of Geology, Geophysics and Mineralogy, Siberian Branch of Russian Academy of Sciences (Novosibirsk, Russia) using standard procedures for controlling accuracy and reproducibility of the analysis. The trace elements were analyzed using an Inductively Coupled Plasma Mass Spectrometer (PerkinElmer/SciexElan 6100 DRC) at the Institute of Mineralogy, Geochemistry and Crystal Chemistry of Rare Earth Elements (Moscow, Russia). Sample preparation was done using a low-pressure HF digestion.

composition is generally assumed to correspond to the composition of the upper continental crust (Taylor and McLennan, 1985). However, compared to PAAS, they are poorer in large-ion lithophile elements (LILE) and light REE (Fig. 5a,b). At the same time, the lithophile element spectra (high values of LILE/HFSE ratios, distinctly pronounced Nb anomalies (Nb/Nb*$=0.49$–0.55) and Ta anomalies (Ta/Ta*$=0.32$–0.37)) in multi-element diagrams, where the mudstone compositions are normalized to the primitive mantle (Fig. 5c), are identical to those in the volcanic rocks of the calc-alkalic series. This result suggests that the mudstones of the terrigenous complex were mainly
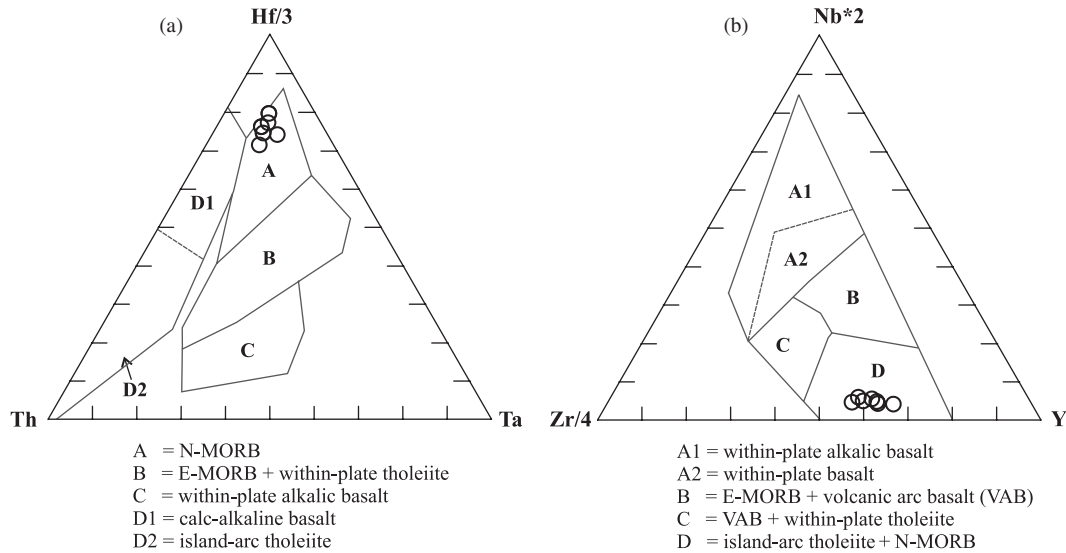
Fig. 4. The Th–Hf–Ta (Wood, 1980) and Y–Nb–Zr (DePaolo and Wasserburg, 1976) discrimination plots demonstrating the similarity of the basalts we studied to N-MORB.

produced by the erosion of upper continental crust. Deviations in the composition of mudstones from that of PAAS were most probably caused by the predominant contribution of volcanics from the active continental margin or from an ensialic island arc.

The composition of mudstones was apparently controlled by variable contributions from several sources, such as, the upper continental crust, reworked sedimentary rocks, a young undifferentiated arc, a young differentiated arc, and exotic components. The high Th/U ratio (3.06–3.77), as well as Th/Sc and Th/Zr ratios, suggest that the sediments were not involved in significant recycling and also imply the insignificant effect of weathering on the composition of the mudstones. High Th/U ratios (3.06–3.77 > 3.0) and negative Eu anomalies (Eu/Eu* = 0.72–0.97) suggest that continental crust made a contribution. However, low Th/Sc (0.35–0.52 ≪ 1) and La/Sc (1.00–1.49 ≪ 4.0) ratios and moderate La/Th ratios (2.844–2.88), in combination with the rather low Hf content (5.29–5.61 ppm), suggest a significant erosion of acid volcanic rocks in an active island arc or along an active continental margin (McLennan et al., 1993). The high Cr/Ni ratios (1.94–2.00), in combination with the elevated vanadium contents (194–257 ppm), indicate erosion of basic volcanic rocks (i.e. Garver and Scott, 1995).

Thus, mudstones of the terrigenous complex were presumably derived from volcanic rocks in an active island arc build on continental crust that was locally dissected. The likely source is compatible with, but not restricted to, the mid-Cretaceous Okhotsk-Chukotka volcanic belt.

4.4. Detrital zircon thermochronology

Cooling ages of detrital zircon from sandstones can provide minimum constraining ages for the time of deposition as well as information about the cooling of

Table 2
Trace-element contents in shales and sandstone of the Omgon Cape

Sample	OM-26/98	OM-36/98	O-28(4)/98
Trace and rare-earth elements (ppm)			
Sc	21	19	13
Ti	5689	5574	6051
V	257	194	96
Cr	116	71	22
Mn	374.02	433.32	376
Co	24	14	13
Ni	60	35	23
Cu	36	34	17
Zn	134	115	58
Rb	66.1	103.4	68.5
Sr	287	136	108
Y	32	36	24
Zr	175	208	171
Nb	11.18	14.75	18.7
Ta	0.58	0.83	0.71
Ba	578	355	704
Hf	5.61	5.29	4.67
Pb	13.55	19.1	10.77
Th	7.20	10.00	6.22
U	2.35	2.65	1.50
La	20.76	28.40	22.50
Ce	55.06	66.32	43.60
Pr	7.84	8.61	6.04
Nd	22.70	28.45	25.07
Sm	5.09	6.29	4.37
Eu	1.71	1.53	1.40
Gd	5.70	6.68	4.19
Tb	0.76	0.97	0.61
Dy	4.96	5.54	4.38
Ho	0.94	1.27	0.86
Er	2.79	3.83	2.15
Tm	0.51	0.55	0.39
Yb	2.54	3.62	2.15
Lu	0.44	0.59	0.33

Sample numbers OM-26/98 and OM-36/98 belong to shales; sample number O-28(4)/98 belongs to sandstone. Also see notes to Table 1.
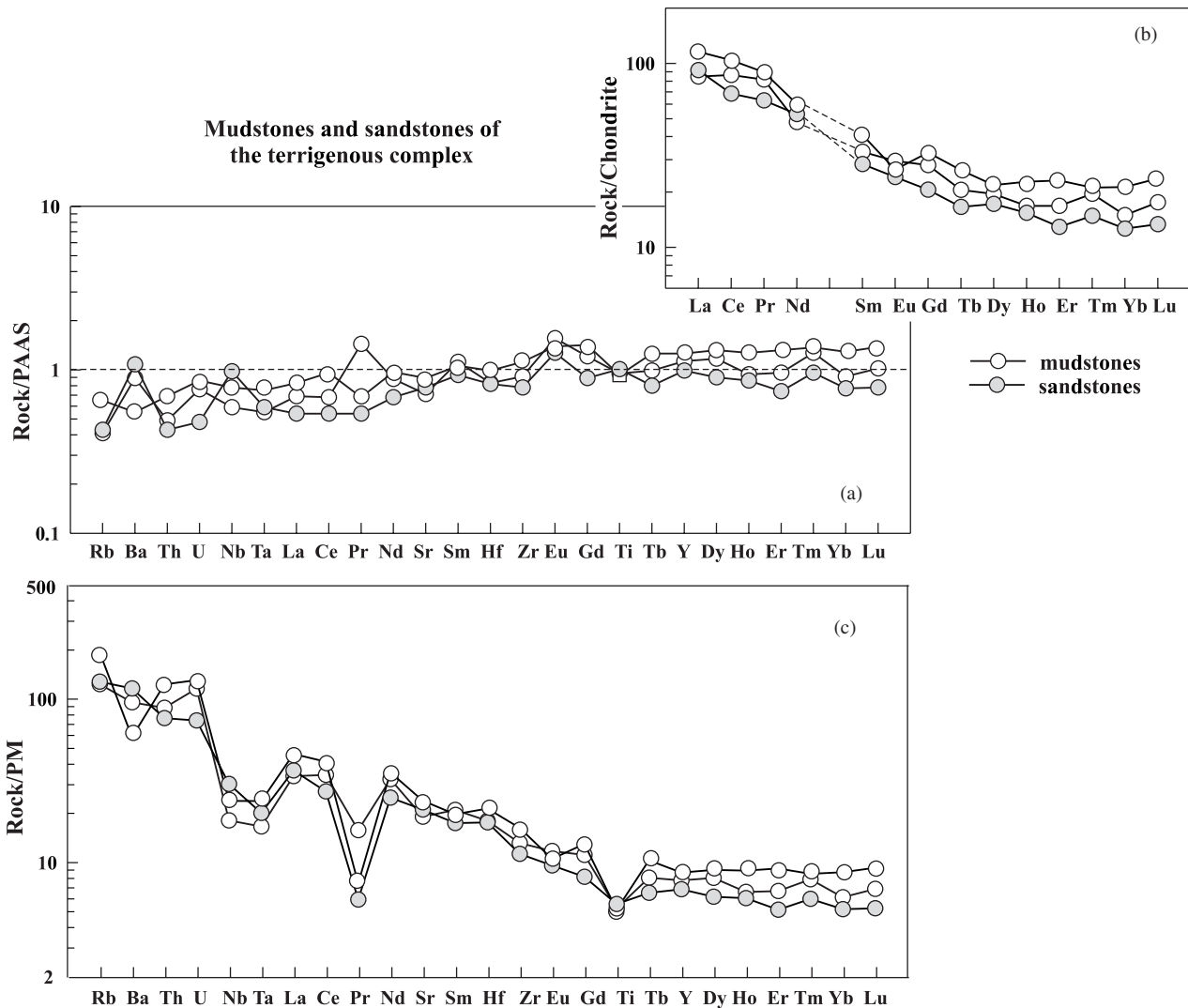
Fig. 5. Multi-element diagrams and REE spectra for the terrigenous rocks of the Omgon Range. Normalized PAAS values are after (Taylor and McLennan, 1985); primitive mantle (PM) values, after Hofmann (1988) and chondrites, after Sun and McDonough (1989).

source terrains (Garver and Brandon, 1994; Garver et al., 1999, 2000; Soloviev et al., 2002a,b; Bernet and Garver, in press). Fauna and flora fossils from these rocks indicate Albian–Santonian deposition for the terrigenous complex (Vlasov, 1964). Detrital zircons were separated from eight samples of sandstones from the terrigenious complex, and from one from the unconformably overlying Eocene strata (Table 3). The ages of individual zircon grains were determined by the external-detector method, and 45–75 zircon grains were dated for each sample (Wagner and Van den Haute, 1992; Garver et al., 1999; see Supplementary material, Table 3, Fig. 6A,B). Our analysis of the distribution of fission-track ages from the terrigenious complex (not for Eocene deposits) determined that the samples have two or three component populations (P) of the following main age groups: P1: 114–80 Ma; P2: 187–142 Ma; and P3: c. 250 Ma. The presence of zircons of various ages in the sandstones, as well as the lack of secondary metamorphic minerals, suggest that the rocks

were not heated above the zircon closure temperature after deposition (approximately 200–240 °C) (Brandon and Vance, 1992; Garver et al., 2005). Hence, it is likely that the ages of the populations reflect the cooling events of the rocks in the source area, and not subsequent heating events.

The youngest population, P1, has an age range of 114.5 ± 7.2–80.0 ± 4.1 Ma (Albian to earliest Campanian; see Fig. 6d). Zircons from the younger population are mainly colorless idiomorphic crystals, which are characteristic, but not diagnostic, of first cycle zircons. These zircons most probably originated from volcanic activity synchronous with the flysch accumulation. It has been demonstrated in a number of papers that the age of the youngest zircon population is close to the age of the rock deposits, provided that volcanic activity occurred in the immediate vicinity of the sedimentary basin at the time of sedimentation (Garver et al., 1999, 2000; Shapiro et al., 2001; Soloviev et al., 2002b; Bernet and Garver, in press). Therefore, rocks of the terrigenous complex accumulated from Albian to earliest

Table 3
Summary of detrital zircon fission-track data

N sample Unit		N_t	Age range (Ma)	P1	P2	P3	P4
The Omgon Range							
OM41	Eocene deposits	42	34–306	45.2 ± 3.2 (39.2%)	68.3 ± 13.0 (17.9%)	101.2 ± 9.7 (35.7%)	293.0 ± 60.7 (7.1%)
OM3	Terrigenous complex	75	56–209	80.0 ± 4.1 (94.6%)	175.7 ± 50.5 (5.4%)		
OM39	Terrigenous complex	74	62–193	85.3 ± 4.2 (95.2%)	167.8 ± 33.6 (4.8%)		
OM30	Terrigenous complex	46	66–254	90.6 ± 9.0 (52.8%)	151.3 ± 17.3 (47.2%)		
OM27	Terrigenous complex	75	67–275	99.8 ± 5.8 (83.2%)	187.0 ± 27.9 (16.8%)		
OM24	Terrigenous complex	75	74–365	102.0 ± 18.9 (18.8%)	142.2 ± 12.0 (68.1%)	248.2 ± 28.8 (13.1%)	
OM22	Terrigenous complex	60	82–423	114.5 ± 7.2 (69.8%)	–	237.1 ± 25.3 (30.2%)	
The Rassoshina River Valley							
OM48	Terrigenous complex	70	62–297	79.5 ± 8.0 (30.0%)	108.0 ± 12.3 (49.6%)	179.3 ± 28.0 (20.5%)	
OM50	Terrigenous complex	65	61–264	77.7 ± 6.6 (49.7%)	96.6 ± 11.4 (46.0%)	198.3 ± 64.8 (4.3%)	

Note. N_t = number of grains; percentage of grains calculated in a specific peak; Age for each population is in Ma, uncertainties cited at $\pm 1\sigma$. Zircons were dated using standard methods for FT dating using an external detector. Mounts were etched in a NaOH–KOH at 228 °C for 15 and 30 h and then irradiated at Oregon State with a fluence of 2×10^{15} n/cm^2, along with zircon standards and dosimeter CN-5. Tracks were counted on an Olympus BX60 at 1600×, and a ζ-factor of 348.2 ± 11.02 was used. Fission-track ages were computed using the program Zetaage 4.7 (Brandon, 1996). To discriminate the populations by age, we used the program Binomfit 1.8 (Brandon, 1996).

Campanian time assuming volcanism was active in the source area.

Samples of sandstones and mudstones were collected in the Rassoshina River Valley (east of the Omgon Range); these rocks are overlain by chert and pillow basalts. Because no fauna remains were discovered in the flysch in these exposures, these FT minimum ages provide the first constraints on their age (see Supplementary material, Table 3, Fig. 6D). The ages of the young population of zircons are 79.5 ± 8.0 and 77.7 ± 6.6 Ma. Note that the sampled flysch sections east of the Omgon Range appear to be somewhat younger than rocks of the terrigenous complex of the Omgon Range.

4.5. Fission-track dating of apatite

Fission-track dating of apatite from sedimentary rocks allows reconstruction of the thermal evolution of the sedimentary deposits after deposition because the annealing temperature of typical apatite is $\sim 110 \pm 5$ °C (Laslett et al., 1987). FT dating of apatite from the sandstones of the terrigenous complex (Table 4) demonstrates that low-temperature cooling occurred between 74 and 58 Ma. Apatite FT ages of 6 samples (OM3, OM22, OM24, OM27, OM30, and OM39) are about 70 Ma, which suggests exhumation and cooling to ~ 100 °C (a depth of c. 4 km with a geothermal gradient of 25 °C/km) during the Maastrichtian. The apatite age from sample OM3 ($57.7 \pm$

7.0 Ma) suggests reheating during a thermal episode associated with local intrusion of a sill (see Table 4).

The Upper Cretaceous flysch deposits (Rassoshina River valley) experienced a different thermotectonic evolution, because they have AFT cooling ages of c. 38 Ma. This young cooling event might have been associated with the transient thermal affects of the Eocene Kinkil volcanic belt (Gladenkov et al., 1991; Soloviev et al., 2002a).

4.6. Cenozoic rocks of the Omgon Range

Numerous differentiated sills (Fig. 2) of basalt, basaltic andesite, andesite, dacite, and rhyolite and their holocrystalline equivalents intrude deposits of the terrigenous rock complex in the northern part of the Omgon Range (Ledneva et al., 2001). The sills were deformed along with the enclosing terrigenous deposits. The age of the sills was determined by the fission-track dating of apatite and zircon (see Table 4), and apparently the sills cooled, and therefore were likely to have been emplaced, in the Late Paleocene (63–60 Ma).

A sandstone sample from the basal horizons of the Eocene Snatol Formation that unconformity overlies the deformed Cretaceous rock (sample OM41) was collected for fission-track dating of zircon. The sample has four populations of cooling ages for detrital zircon (see Table 3, Fig. 6C). The youngest population of zircons from the sandstone is 45.2 ± 3.2 Ma (Middle Eocene),
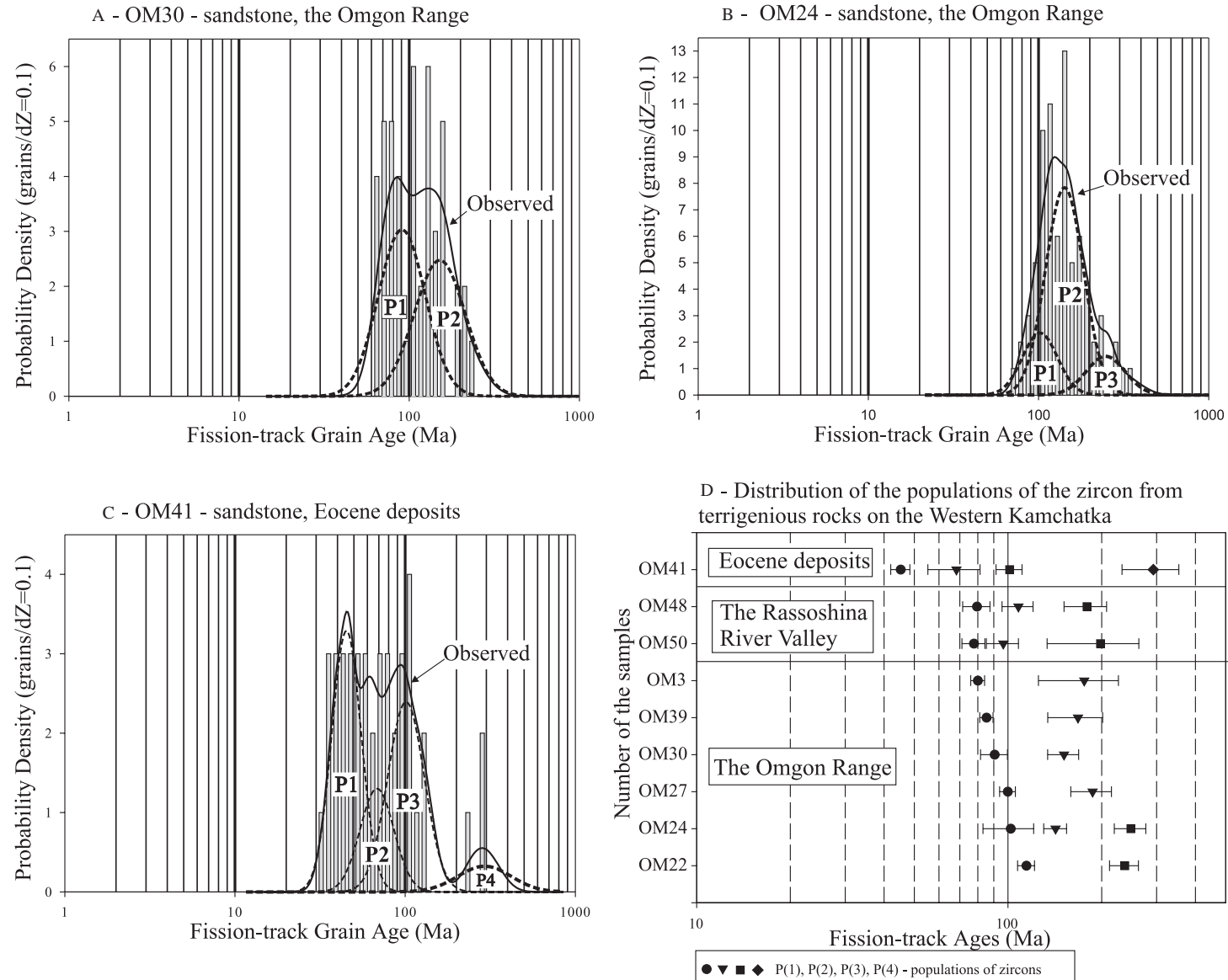
Fig. 6. Probability density plots (A, B and C with histograms) for representative fission-track grain-age distributions from the Omgon Range (Western Kamchatka). Thick lines show probability density distribution, and dashed lines show the best-fit peaks, as reported in Table 3. The fission-track minimum age corresponds to the age of the youngest peak. Plots were constructed according to Brandon (1996). Age is plotted on a logarithmic axis. The probability density scale is the same for both the density plots and the histograms. Density units are given relative to dZ=0.1, which corresponds to an interval on the age scale approximately equal to 10% of the age. Plot (D) of fission-track zircon results for sandstone from Western Kamchatka (Table 3). Circles—minimum ages (young population P1), triangles (P2), squares (P3), rhomb (P4)—older peak ages, respectively. Error bars show the 63% confidence intervals.

Table 4
Apatite and zircon fission-track data

No. sample	Unit	Elev (m)	ρ_s	N_s	ρ_i	N_i	ρ_d	n	χ^2	Age	$-/+1\sigma$	U (ppm) $\pm 2\sigma$
Omgon range												
Zircon												
O98-27	Sill (gabbro)	10	68.5	1766	5.03	1296	0.27	30	99.4	62.5	−3.3+3.5	231.0±17.8
O98-43	Sill (gabbro)	15	105.0	1116	8.42	891	2.92	17	100.0	63.0	−3.8+4.0	350.9±32.7
Apatite												
O98-27	Sill (gabbro)	10	4.51	222	1.12	551	2.93	15	100.0	60.9	−6.7+7.6	15.2±1.4
OM3	Terrigenous	5	3.53	194	0.76	419	3.10	20	98	73.9	−8.5+9.6	9.8±1.0
OM22	Terrigenous	7	4.02	101	0.96	241	3.08	15	49.8	66.5	−9.0+10.4	12.4±1.7
OM24	Terrigenous	3	2.76	130	0.44	209	3.06	15	0.2	73.7*	−12.8+15.5	5.8±0.8
OM27	Terrigenous	7	2.04	91	0.45	201	3.05	15	97.5	71.3	−8.3+9.2	5.9±0.9
OM30	Terrigenous	150	3.93	168	0.86	367	3.03	15	80.8	71.5	−8.5+9.6	11.3±1.3
OM39	Terrigenous	0	4.38	247	1.18	665	3.01	25	80.3	57.7	−6.2+7.0	15.6±1.4
Rassoshina River												
OM48	Terrigenous	150	4.77	282	1.39	822	2.98	26	0.0	37.6*	−6.1+7.3	18.6±1.5
OM50	Terrigenous	150	7.78	166	1.64	349	2.96	15	0.0	38.0*	−7.8+9.8	22.0±2.5

Note. In this table ρ_s is the density (cm^2) of spontaneous tracks ($\times 10^5$) and N_s is the number of spontaneous tracks counted; ρ_i is the density (cm^2) of induced tracks ($\times 10^6$); and ρ_d is the density (cm^2) of tracks on the fluence monitor ($\times 10^6$); n is the number of grains counted; and χ^2 is the Chi squared probability in percent. Fission-track ages ($\pm 1\sigma$) were calculated using the ζ-method, and ages were calculated using the computer program and equations in (Brandon, 1996). The ζ-factors were 104.32 ± 3.35 (for apatite based on CN1 calibration) and 348.2 ± 11.02 (for zircon based on CN5 calibration). All ages that pass χ^2 (>5%) are reported as pooled ages, otherwise first population ages calculated by BinomFit 1.8 (Brandon, 1996; Brandon, 2002) are shown (denoted by *). Glass (CN-1) monitors, placed at the top and bottom of all irradiation packages (for ζ calculations) were used to determine the fleunce gradient in each package. After etching, mounts were covered with a low-uranium mica detector, and irradiated with thermal neutrons at Oregon State University with a nominal fluences of 8×10^{15} n/cm^2 (for apatite) and 2×10^{15} n/cm^2 (for zircon), along with a standards (Fish Canyon Tuff, Buluk Tuff) and a reference glass dosimeter CN1 (for apatite) and CN5 (for zircon). All samples were counted at 1600× using a dry 100× objective (10 oculars and 1.6× multiplication factor) on Olympus BX60 microscope fitted with an automated stage and a Calcomp digitizing tablet.

which is equivalent to the known stratigraphic age of the unit (Soloviev et al., 2001).

5. Interpretation

A basic conclusion from our study is that Jura-Cretaceous oceanic volcanics are tectonically mixed with mid-Cretaceous continental margin sediments in a structural complex formed during the latest Cretaceous. Volcanic rocks of the Omgon Range formed during the latest Jurassic–Early Cretaceous in an oceanic or marginal sea setting. Basalts of this complex are comparable with N-MORB from oceanic-type spreading centers. It is possible that the paleo-Pacific-Izanagi plate (Engebretson et al., 1985) was the source of the volcanic blocks.

Terrigenous rocks accumulated as turbidites in submarine fans during the Albian to the Campanian in a continental-margin environment. The composition of the mudstones and sandstones suggest the source was a dissected volcanic arc, probably the Okhotsk-Chukotka volcanic belt, which was built on continental basement of the Eurasian margin. Blocks and slides of the volcanic rocks have tectonic contacts with the terrigenous rocks, which make up the matrix of the succession.

Thus, rocks of different ages that were formed in different geodynamic settings are tectonically mixed. This

mixing of oceanic lithologies within a matrix of terrigenous rocks suggests that the rock units of the Omgon Range are part of an accretionary prism. In this scenario, slides and blocks of oceanic origin were accreted during subduction and mixed with the terrigenous Albian–earliest Campanian deposits of the continental-margin.

Fission-track dating of apatite suggests that this accretionary prism was exhumed to a near-surface level (<c. 4 km) by the Maastrichtian ($\sim$70 Ma), about 10–20 Myr after deposition. FT ages of zircon and apatite from felsic sills shed light on the level of exhumation of the accretionary complex in the Late Cretaceous. Most of the cooling ages (both ZFT and AFT) fall between 60 and 70 Ma (Table 4), and some ZFT and AFT ages are nearly concordant (i.e. sample 098–28), which suggests that at that time, the enclosing rocks were at relatively shallow levels (<4 km). Intrusion of the felsic dikes and sills probably marked the end of accretion of material in this system. If this is the case, the accretion process had been completed by the Late Cretaceous, and rocks of the Omgon Range were incorporated into the structure of the continental margin. In the Late Paleocene, sills and dikes intruded into the accretionary prism at a latitude close to the present-day position of the Omgon Range as indicated by paleomagnetic studies (Chernov and Kovalenko, 2001). This intrusion signals an extremely important oceanward shift in the locus of arc magmatism in the latest Cretaceous to Early Tertiary.

6. Regional setting

An important aspect of paleogeographic reconstructions is the regional distribution of arc and forearc complexes along the NE Eurasian margin. Previous studies have not fully investigated the lateral continuity of Cretaceous accretionary complexes along the northeastern Eurasian margin. This lack of analysis is partly due to discontinuity of exposures in remote, difficult to access locations. Because exposures are limited, there is considerable uncertainty in tectonic reconstructions for the evolution of the northeast Eurasian margin in the Cretaceous. Here we try to fill this gap by piecing together relics of the Cretaceous accretionary complexes along the NW Eurasian margin.

Throughout much of the northwestern Pacific, accumulation of terrigenous strata commenced in the Albian in basins genetically associated with subduction under the Eastern-Asian volcanic belt (Belyy, 1977; Filatova, 1988; Zonenshain et al., 1990; Belyy, 1994; Hourigan and Akinin, 2004). The Eastern-Asian volcanic belt is a laterally extensive Andean-style arc subdivided into different sectors based on differences in the basement rock types and lithologic similarity of volcanic sections within specific geographic regions (Belyy, 1977; Melankholina, 2000) (Fig. 7). From north to south these sub-divisions include: Chukotka–Alaska, Okhotsk-Chukotka, Eastern Sikhote-Alin, and Korea–Japan. Terrigenous sedimentation occurred in syn-subduction forearc basins along the eastern Eurasian margin (Melankholina, 2000; Garver et al., 2000; Shapiro et al., 2001; Soloviev et al., 2001; Zharov, 2003). These basins include, from north to south, the Bering Sea basin, Ukelayat basin, North Okhotsk basin, Western Kamchatka basin, Western Sakhalin basin, Ieso basin, and the Shimanto basin. Clastic rocks in these basins accumulated in slightly different tectonic settings, but all record erosion of the arc and deposition along the continental margin. Continental and shallow-water forearc basins, and post-Albian molasse deposits, are known in the Pendzhina and Northern Korayk regions (Zinkevich, 1981; Filatova, 1988; Sokolov, 1992). The Albian–Campanian forearc basin deposits have been described in the Penzhina Guba (Bay) area northwest of northern Kamchatka (Tuchkova et al., 2003). The Western Sakhalin and Ieso forearc basins (Fig. 7) contain Aptian–Paleocene clastic deposits derived from the Eastern Sikhote-Alin volcanic belt (Melankholina, 2000; Zharov, 2003).

The continent-derived flysch with exotic ocean-derived blocks is typical and are interpreted to have been imbricated in accretionary wedges along the continental margin (i.e. Cowan, 1985). The relics of the accretionary wedge related to Cretaceous subduction are known in the following segments of the present-day tectonic framework of the eastern Eurasian margin (Fig. 7): Yanranai (Korayk Upland) (Grigor'ev et al., 1987; Sokolov, 1992), Omgon (Western Kamchatka) (this study), Tonino–Aniva (southeastern Sakhalin) (Zharov, 2003), Hidaka (Kiminami et al., 1992; Zharov, 2003) and Shimanto (Taira et al.,
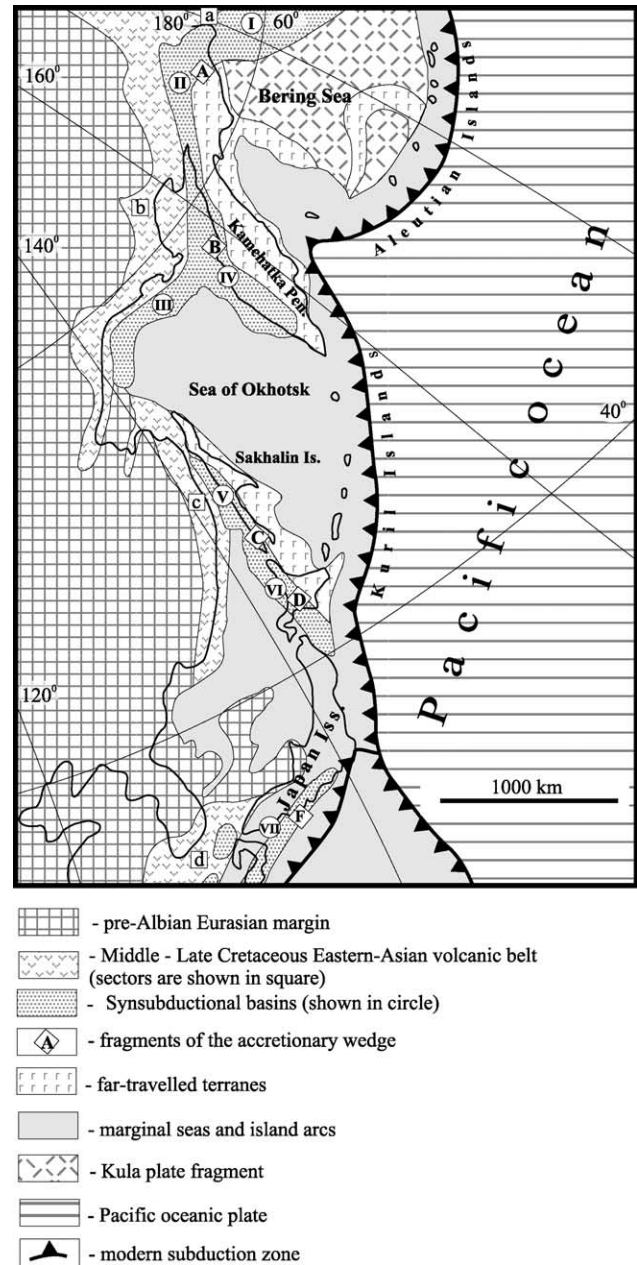

Fig. 7. Tectonic elements of the mid- to Late-Cretaceous margin within the context of the modern setting of northeastern eurasia (Melankholina, 2000). Outlined letters (Squares) represent the following sectors of the mid- to Late Cretaceous Eastern-Asian volcanic belt: a, Chukotka-Alaska; b, Okhotsk-Chukotka; c, Eastern Sikhote-Alin; d, Korea-Japan. Numbers in circles are syn-subduction basins: I, Bering Sea; II, Ukelayat; III, North Okhotsk basin; IV, Western Kamchatka basin; V, Western Sakhalin basin; VI, Ieso basin; VII, Shimanto basin. Letters in rhombohedra are fragments of the accretionary wedge: A, Yanranai; B, Omgon; C, Tonino–Aniva; D, Hidaka; F, Shimanto.

1988). Hence, we are impressed not only by the similarity of these units, but also the apparent lateral continuity of this N–S petrotectonic assemblage. We review the occurrences of these rocks below, starting in the north and working southward.

The three tectonic slices were described in the Yanranai accretionary complex in the Koryak upland of northern Kamchatka (from Grigor'ev et al., 1987; Sokolov, 1992). The slices consist of oceanic crust fragments with different ages, but younger rocks have a lower structural position. The terrigenous rocks, inferred to have been derived from the Eurasian margin, occur in the upper part of the each slice. The accretion of the Jurassic–Neocomian oceanic rocks, presumably part of the Izanagi or Kula plate, occurred at the end of the Early Cretaceous. The second stage of accretion was at the end of the Late Cretaceous. The final stage was completed in the Maastrichtian when an olistostrome unit formed.

Rocks of the Tonino–Aniva Peninsula (southeastern Sakhalin Island, western part of the Sea of Okhotsk) are inferred to have accumulated in an accretionary prism (Zharov, 2003). The Tonino–Aniva complex consists of a mid-Cretaceous turbidite and olistostrome unit with tectonic slivers of volcanic rocks inferred to be fragments of a Jurassic–Lower Cretaceous seamount. The structural lower part of the complex is represented by Upper Cretaceous turbidites. The Tinino-Aniva complex is inferred to have formed as a result of Aptian–Cenomanian subduction of the Sorachi oceanic plateau and syn-accretionary turbidites in the Late Cretaceous.

Farther south, the Hidaka terrane on Hokkaido Island (Japan), has been described as a Late Cretaceous–Early Eocene accretionary wedge (Kiminami et al., 1992; Zharov, 2003). The terrane contains continental-derived terrigenous mélange that is probably a dismembered turbidite complex with an eastern structural vergence. The change from hemipelagic rocks low in the section to clastic rocks higher in the sequence shows that the depositional setting varied from abyssal plain to continental margin.

The best-studied example of the accretionary wedge from the entire belt is the Shimanto (Taira et al., 1988; Suzuki, 1988; Matsumoto et al., 1988; Hasebe et al., 1993; Hashimoto and Kimura, 1999; Hasebe and Tagami, 2001). The Shimanto Belt has an overall younging trend from north to south (Taira et al., 1988), but here we are mainly concerned with the older part of the belt that is similar in age to those to the north. The Upper Cretaceous part of the Shimanto Belt includes turbiditic sandstone and shale and minor conglomerate interbedded with hemipelagic varico-lored shale. The biostratigraphic ages from the flysch unit range from Coniacian to Campanian. Mélange, which occurs as several linear belts sandwiched between flysch units, is composed of a highly deformed argillaceous 'matrix' with various-sized tectonic slivers. The tectonic slivers include pillow basalts, chert, and varicolored shale. A remarkably constant age-lithology relationship occurs in this unit: the tectonic slivers contain dated rocks from the Tithonian to Cenomanian, and the sheared argillaceous matrix yields mostly Campanian radiolaria (Taira et al., 1988). Most of the meta-basalts in the Shimanto mélange zones are considered to have originally been ocean-floor

basalts (MORB), but also include alkali basalts possibly derived from volcanic islands or seamounts (Suzuki, 1988). The overwhelming geological evidence suggests that the Shimanto Belt is an accretionary prism of Cretaceous to Tertiary age (Taira et al., 1988). The contemporaneous Cretaceous volcano-plutonic belt is distributed along a linear belt extending from Japan to Shikhote Alin to the north. This same plutonic belt can be traced northward into the Okhotsk-Chukotka volcanic belt (OCVB).

Our new data suggest that the Omgon accretionary complex belongs to this family of mid to Upper Cretaceous accretionary complexes that accumulated along the NW Pacific margin (Fig. 7). The Omgon is similar to the Yanranai (northern Koryak), Tonino–Aniva (southeastern Sakhalin), Hidaka (northeastern Japan) and Cretaceous Shimanto belt (southwestern Japan) in age, structure and tectonic position. Together, these accretionary complexes record Cretaceous subduction under northeastern Eurasian, assuming there has not been significant tectonic translation along the margin. One important aspect to note about this family of accretionary complexes is that the ones farthest south (Japan) appear to have continued from the Cretaceous to Eocene, but to the north there is no evidence of this complex having ages younger than the Cretaceous. It is possible that this difference can be attributed to accretion and outboard jump in accretion after the Cretaceous in the northern areas.

The Omgon accretionary complex separated from the Okhotsk-Chukotka volcanic belt due to extension of the Sea of Okhotsk, the evolution of which is poorly known (see geological overview). We speculate that our new data are consistent with the back-arc extensional model of the origin of the Sea of Okhotsk (Hourigan, 2003). The basement rocks of the Sea of Okhotsk are inferred to be comprised of a variety of terranes that were rifted apart since the Eocene. One terrane is the Omgon accretionary complex and presumably an inboard forearc basin.

7. Conclusions

The Omgon Range in Western Kamchatka is composed of southeast-verging interleaved tectonic units imbricated in a subduction setting. Sandstones are uniform in composition and the sediment is inferred to have been derived from a continental arc. FT depositional ages of detrital zircons from the Omgon flysch are Albian–Campanian, which is similar to the depositional age inferred from fossils. It is likely that this arc that supplied terrigenous sediments was the contemporaneous Okhotsk-Chukotka volcanic belt partly because the main phase of volcanism and plutonism in this belt occurred during the mid-Cretaceous. The flysch is clearly imbricated with older oceanic rocks. The basalts are tholeites similar to those associated with spreading centers within oceanic and marginal basins, and the overlying siliceous rocks are Upper Jurassic to Lower Cretaceous in age. The Albian–Campanian continent-derived flysch with

the exotic Upper Jurassic to Lower Cretaceous ocean-derived blocks is a relict of the accretionary wedge related to Cretaceous subduction under the Eurasian margin. Internal imbrication of the Omgon complex was complete by the Maastrichtian ($\sim$70 Ma) when apatite fission-track cooling ages were recorded.

Other accretionary complexes to the north (northern Kamchatka) and to the south (Japan) consist of a broadly coeval terrigenous matrix and oceanic blocks, the blocks being older than the matrix. We suggest that these disparate occurrences of mid to Upper Cretaceous accretionary complexes retain a record and the gross position of the subduction zone along the Eurasian margin. Cretaceous to Eocene ages of matrix rocks to the south may indicate that the subduction zone operated continuously to the south, but was interrupted to the north. We speculate that the Omgon accretionary complex was separated from the Okhotsk-Chukotka volcanic belt by extension that occurred during formation of the Sea of Okhotsk since Eocene time.

Acknowledgements

Appendix. Supplementary material

Supplementary data associated with this article can be found, in the online version, at doi:10.1016/j.jseaes.2005.04.009

References

Belyy, V.F., 1977. Stratigraphy and Structure of the Okhotsk-Chukchi Volcanic Belt. Nauka, Moscow, p. 275 (in Russian).

Belyy, V.F., 1994. Geology of the Okhotsk-Chukotka volcanic belt Magadan, NEISRI REB RAS, p. 76 (in Russian).

Bernet, M., Garver, J.I., in press, Chapter 8: Fission-track analysis of Detrital zircon, In: P.W. Reiners, T. Ehlers, (Eds.), Low-Temperature Thermochronology, Reviews in Mineralogy and Geochemistry Series.

Bogdanov, N.A., Chekhovich, V.D., 2002. On the collision between the West Kamchatka and sea of Okhotsk plates. Geotektonika 1, 63–76 (in Russian).

Bogdanov, N.A., Dobretsov, N.L., 2002. The Okhotsk volcanic plateau. Russian Geology and Geophysics (English Translation) 43 (2), 87–99.

Bogdanov, N.A., Bondarenko, G.E., Vishnevskaya, V.S., Izvekov, I.N., 1991. The middle–upper Jurassic and lower cretaceous radiolarian assemblages in the Omgon range (Western Kamchatka). Transactions (Doklady) of the USSR Academy of Sciences, Earth Science Sections 321 (2), 344–348.

Bondarenko, G.E., Sokolkov, V.A., 1990. New data on the age, structure, and genesis of volcanic–Cherty–carbonate complex on Cape Omgon (West Kamchatka). Transactions (Doklady) of the USSR Academy of Sciences, Earth Science Sections 315 (6), 1434–1437.

Brandon, M.T., 1996. Probability density plot for fission-track grain-age samples. Radiation Measurements 26 (5), 663–676.

Brandon, M.T., 2002. Decomposition of mixed grain-age distributions using BINOMFIT. On Track 24, 13–18.

Brandon, M., Vance, J., 1992. Tectonic evolution of the Cenozoic Olympic subduction complex, western Washington State, as deduced from fission track ages for detrital zircon. American Journal of Science 292, 565–636.

Brandon, M.T., Roden-Tice, M.R., Garver, J.I., 1998. Late Cenozoic exhumation of the Cascadia accretionary wedge in the Olympic Mountains, northwest Washington State. GSA Bulletin 100, 985–1009.

Chernov, E.E., Kovalenko, D.V., 2001. Paleomagnetism of geologic complexes in the Omgon range (West Kamchatka Coast). Physics of the Solid Earth 37 (5), 68–77.

Cowan, D.S., 1985. Structural styles in Mesozoic and Cenozoic mélanges in the western Cordillera of North America. GSA Bulletin 96, 451–462.

DePaolo, D.J., Wasserburg, G.J., 1976. Inference about magma sources and mantle structure from variations of 143Nd/144Nd. Geophysics Research Letters 3, 743–746.

Dumitru, T., 1989. Constraints on the uplift of the Franciscan subduction complex from apatite fission track analysis. Tectonic 8, 197–220.

Engebretson, D.C., Cox, A., Gordon, R., 1985. Relative motions between oceanic and continental plates in the Pacific Basin. Geological Society of America, Special Paper 206, 59.

Filatova, N.I., 1988. Peri-Oceanic Volcanic Belts. Nedra Publishers, Moscow, p. 262 (In Russian).

Garver, J.I., Brandon, M.T., 1994. Fission-track ages of detrital zircon from Mid-Cretaceous sediments of the Methow-Tyaughton Basin, Southern Canadian Cordillera. Tectonics 13 (2), 401–420.

Garver, J.I., Scott, T.J., 1995. Rare earth elements as indicators of crustal provenance and terrane accretion in the southern Canadian Cordillera. GSA Bulletin 107 (4), 440–453.

Garver, J.I., Brandon, M.T., Roden-Tice, M., Kamp, P.J.J., 1999. Exhumation history of Orogenic highlands determined by detrital fission-track thermochronology. In: Ring, U., Brandon, M.T., Lister, G.S., Willett, S.D. (Eds.), Exhumation Processes: Normal Faulting, Ductile Flow and Erosion Geological Society London, Special Publications, vol. 154, pp. 283–304.

Garver, J.I., Soloviev, A.V., Bullen, M.E., Brandon, M.T., 2000. Towards a more complete record of magmatism and exhumation in continental arcs, using detrital fission-track thermochronometry. Physical Chemistry Earth Part A 25 (6–7), 565–570.

Garver, J.I., Reiners, P.R., Walker, L.J., Ramage, J.M., Perry, S.E., 2005. Implications for timing of Andean uplift based on thermal resetting of radiation-damaged zircon in the Cordillera Huayhuash, northern Perú. Journal of Geology 113 (2), 117–138.

Gladenkov, Yu.B., Sinel'nikova, V.N., Shantser, A.E., Chelebaeva, A.I., Oleinik, A.E., Titova, L.V., Brattseva, G.M., Fregatova, N.A., Zyryanov, E.V., Kazakov, K.G., 1991. The Eocene of Western Kamchatka. Nauka Publishers, Moscow, p. 181 (In Russian).

Grigor'ev, V.N., Krylov, K.A., Sokolov, S.D., 1987. Jurassic and Cretaceous Deposits of Yanranai Accretionary Complex (Koryak Highland) Essays on the Geology of the Northwestern Pacific Belt. Nauka Publishers, Moscow, p. 132–159 (In Russian).

Grigor'ev, V.N., Sokolov, S.D., Krylov, K.A., Golozubov, V.V., Pral'nikova, I.E., 1995. Geodynamic Types of Triassic–Jurassic Volcanic–Cherty Rock Complexes of the Kuyul Terrane (Koryak Highland). Geotektonika 3, 59–69 (in Russian).

Hasebe, N., Tagami, T., 2001. Exhumation of an accretionary prism—results from fission track thermochronology of the Shimanto Belt, southwest Japan. Tectonophysics 331, 247–267.

Hasebe, N., Tagami, T., Nishimura, S., 1993. Evolution of the Shimanto accretionary complex: a fission-track thermochronologic study. In: Underwood, M.B. (Ed.), Thermal Evolution of the Tertiary Shimanto Belt, Southwest Japan: An Example of Ridge-Trench Interaction, Boulder, Colorado, Geological Society of America Special Paper, pp. 121–136.

Hashimoto, Y., Kimura, G., 1999. Underplating process from mélange formation to duplexing: Example from the Cretaceous Shimanto Belt, Kii Peninsula, southwest Japan. Tectonics 18 (1), 92–107.

Hofmann, A.W., 1988. Chemical Differentiation of the Earth: Relationship Between Mantle, Continental Crust, and Oceanic Crust. Earth Planet Science Letters 90, 297–314.

Hourigan, J.H., 2003. Mesozoic–Cenozoic Tectonic and Magmatic Evolution of the Northeast Russian Margin. PhD Thesis. Stanford University, p. 234.

Hourigan, J.H., Akinin, V.V., 2004. Tectonic and chronostratigraphic implications of new 40Ar/39Ar geochronology and geochemistry of the Arman and Maltan-Ola volcanic fields Okhotsk–Chukotka volcanic belt, northeastern Russia. GSA Bulletin 116 (5/6), 637–654.

Khanchuk, A.I., 1985. Evolution of the Old Sialic Crust in the Arc System of the Eastern Asia. Nauka publishers, Vladivostok, p. 135 (in Russian).

Khanchuk, A.I., Grigor'ev, V.N., Golozubov, V.V., et al., 1990. Kuyul Ophiolitic Terrane. Vladivostok, Daln.-Vost. Otd. Akad. Nauk SSSR, 108 pp. (in Russian).

Kiminami, K.K., Niida, K., Ando, H., Kito, N., Iwata, K., Miyashita, S., Tajika, J., Sakakibara, M., 1992. Cretaceous–Paleocene Arc–trench Systems in Hokkaido; Paleozoic and Mesozoic Terranes: Basement of the Japanese Island Arcs 29th IGCP Field Trip Guide Book. Geological Survey of Japan, Tsukuba, p. 1.

Kirillova, G.L., Kiriyanova, V.V., 2003. J/K boundary in southeastern Russia and possible analogue of the Tetori Group. Memoir of the Fukui Prefectural Dinosaur Museum 2, 75–102.

Konstantinovskaia, E.A., 2001. Arc-continent collision and subduction reversal in the Cenozoic evolution of the Northwest Pacific; an example from Kamchatka (NE Russia). In: Lallemand, S., Liu, C.-S., Angelier, J., Tsai, Y.B. (Eds.), Active Subduction and Collision in Southeast Asia (SEASIA), pp. 75–94.

Kotlyar, I.N., Zhulanova, I.A., Pusakova, T.B., Gagieva, A.M., 2001. Isotopic Systems: Magmatic and Metamorphic Complexes of Northeast Russia. North East Interdisciplinary Scientific Research Institute, Far East Branch, RAS, Magadan p. 319 (in Russian).

Laslett, G.M., Green, P.F., Duddy, I.R., Gleadow, A.J.W., 1987. Thermal Annealing of Fission Tracks in Apatite. Chemistry Geology, Isotope Geoscience Section 65 (1), 1–13.

Ledneva, G.V., 2001. Paleocene Calc-Alkalic Magmatism in Western Kamchatka (with Reference to Cape Omgon) Modern Problems of Geotectonics. Nauchnyi Mir Publishers, Moscow, pp. 28–32 (in Russian).

Markovsky, B.A., 1989. Geological Map of the USSR. Scale 1: 1 000 000 (New Series). Quadrangle 0-57, (58). Palana. Explanatory Note. Leningrad, Vses. Geol. Inst. (in Russian).

Matsumoto, R., Minai, Y., Okamura, M., 1988. Geochemistry and depositional enviroments of bedded chert of the Cretaceuos Shimanto Group, Shikoku, southwest Japan. Modern Geology 12, 197–224.

McLennan, S.R., Hemming, S., McDaniel, D.K., Hanson, G.N., 1993. Geochemical Approaches to Sedimentation, Provenance and Tectonics. In: Johnson, M.J., Basu, A. (Eds.), Processes Controlling the Composition of Clastic Sediments Geological Society of America. Special Paper, vol. 283, pp. 21–40.

Melankholina, E.N., 2000. Late Cretaceous Island–arc zones of the Eastern Margin of Eurasia: geologic-geochemical and tectonic correlation. Geotektonika 3, 41–57 (In Russian).

Nokleberg, W.J., Parfenov, L.M., Monger, J.W.H., Norton, I.O., Khanchuk, A.I., Stone, D.B., Scholl, D.W., Fujita, K., 1998. Phanerozoic tectonic evolution of the circum-north Pacific, US Geological Survey Open File Report 98-754.

Parfenov, L.M., Natal'in, B.A., 1977. Mesozoic–Cenozoic tectonic evolution of northeastern Asia: transactions (Doklady) of the USSR Academy of Sciences. Earth Science Sections 235 (1-6), 89–91.

Shapiro, M.N., Soloviev, A.V., Garver, J.I., Brandon, M.T., 2001. Sources of zircons in the Cretaceous and Paleogene clastics of the West Kamchatka-Ukelayat Zone. Lithology and Mineral Resources 4, 374–389.

Shutov, V.D., Kossovskaya, A.G., Murav'ev, V.I., et al., 1972. Graywackes. Nauka Publishers, Moscow, p. 346 (In Russian).

Silantyev, S., Sokolov, S., Bondarenko, G., Morozov, O., Bazylev, B., Palandzhyan, S., Ganelin, A., 2000. Geodynamic setting of the high-grade amphibolites and associated igneous rocks from the accretionary complex of Povorotny Cape, Northeast Russia. Tectonophysics 325, 107–132.

Sokolov, S.D., 1992. Accretionary Tectonics of the Koryak-Chukchi Segment of the Pacific Belt. Nauka Publisher, Moscow, p. 181 (In Russian).

Sokolov, S.D., Bondarenko, G.E., Morozov, O.L., Aleksyutin, M.V., Palandzhyan, S.A., Khudolei, A.K., 2001. Specific structural features of Paleoaccretionary prisms with reference to Taigonos peninsula (North-East Russia). Transactions (Doklady) of the Academy of Sciences, Earth Science Sections 377 (6), 807–811.

Soloviev, A.V., Lander, A.V., Garver, J.I., Palechek, T.N., Ledneva, G.V., Verzhbitskii, V.E., 2001. Structure and Age of Rocks in the Omgon Range (Western Kamchatka) Modern Problems of Geotectonics. Nauchnyi Mir Publishers, Moscow, pp. 35–40 (in Russian).

Soloviev, A.V., Shapiro, M.N., Garver, J.I., 2002a. Lesnaya nappe, Northern Kamchatka. Geotectonics 36 (6), 469–482.

Soloviev, A.V., Shapiro, M.N., Garver, J.I., Shcherbinina, E.A., Kravchenko-Berezhnoy, I.R., 2002b. New age data from the Lesnaya Group: a key to understanding the timing of arc–continent collision, Kamchatka, Russia. Island Arc 11, 79–90.

Stavsky, A.P., Chekhovich, V.D., Kononov, M.V., Zonenshain, L.P., 1990. Plate tectonics and palinspastic reconstruction of the Anadyr-Koryak region, northeast USSR. Tectonics 9 (1), 81–101.

Stewart, R.J., Brandon, M.T., 2004. Detrital zircon fission-track ages for the 'Hoh Formation': implications for late Cenozoic evolution of the Cascadia subduction wedge. GSA Bulletin 116 (1/2), 60–75.

Sun, S.S., McDonough, W.F., 1989. Chemical and Isotopic systematics of oceanic basalts: implication for mantle composition and processes. In: Saunders, A.D., Norry, M.J. (Eds.), Magmatism in the Oceanic Basins Geological Society Special Publications, vol. 42, pp. 313–345.

Suzuki, T., 1988. Geochemistry of metabasalts in the Shimanto Belt. Modern Geology 12, 225–241.

Taira, A., Katto, J., Tashiro, M., Okamura, M., Komada, K., 1988. The Shimanto Belt in Shikoku, Japan—evolution of cretaceous to miocene accretionary prism. Modern Geology 12, 5–46.

Taylor, S.R., McLennan, S.M., 1985. The Continental Crust: Its Composition and Evolution. Blackwell Publisher, London, p. 312.

Tuchkova, M.I., Markevich, P.V., Krylov, K.A., Koporulin, V.I., Grigor'ev, V.N., 2003. Cretaceous rocks of the Penzhina bay: mineralogy, petrography, and geodynamic sedimentation conditions. Lithology and Mineral Resources 38 (3), 237–250.

Vishnevskaya, V.S., Bogdanov, N.A., Bondarenko, G.E., 1999. Middle Jurassic to Early Cretaceous Radiolaria from the Omgon Range, Western Kamchatka. Ofioliti 24 (1), 31–42.

Vlasov, G.M. (Ed.), 1964. Geology of the USSR. XXXI Kamchatka and the Kuril and Komandorskie Islands. Nedra Publishers, Moscow (in Russian).

Wagner, G.A., Van den Haute, P., 1992. Fission-Track Dating. Kluwer Publishers, Dordrecht, p. 285.

Watson, B.F., Fujita, K., 1985. Tectonic evolution of Kamchatka and the Sea of Okhotsk implications for the Pacific Basin. In: Howell, D.G. (Ed.), Tectonostratigraphic Terranes of the Circum-Pacific Region Circum-Pacific Council for Energy and Mineral Resources, pp. 333–348.

Wood, D.A., 1980. The application of a Th-Hf-Ta diagram to problems of tectomagmatic classification and to establishing the nature of crustal contamination of basaltic lavas of the British Tertiary volcanic province. Earth Planet Science Letters 50, 11–30.

Zharov, A.E., 2003. The geological structure and the Cretaceous-Paleogene geodynamics of the south-eastern Sakhalin. PhD Thesis. Moscow, Geological Institute RAS, p. 301 (in Russian).

Zinkevich, V.P., 1981. Formations and Stages of Tectonic Development of the Korayk Upland North. Nauka, Moscow, p. 112 (in Russian).

Zonenshain, L.P., Kuzmin, M.I., Natapov, L.M., Page, B.M., 1990. Geology of the USSR: a plate-tectonic synthesis. American Geophysical Union, Geodynamics Series 21, 242.